**Supplemental information for:**

# Optically stimulated luminescence dating of Ocean Drilling Program Core 658B: Complications arising from authigenic uranium uptake and lateral sediment movement.

Simon J. Armitage

## Figure

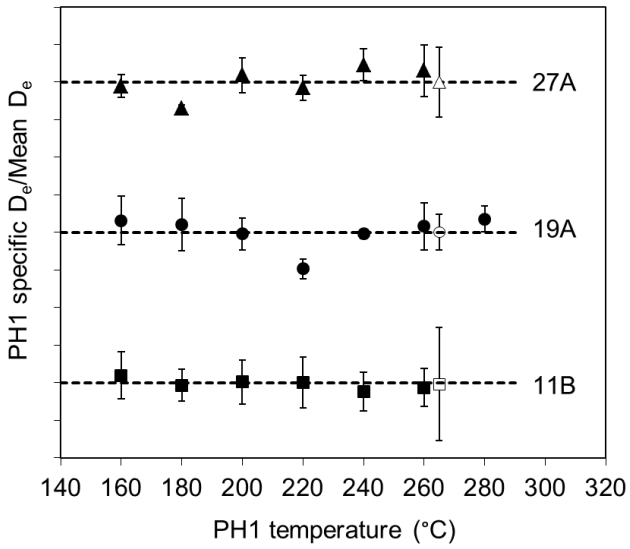


**Figure S1:** Equivalent dose ($D_e$) versus PH1 temperature measured using coarse silt samples. Each point is the mean of two aliquots. Solid markers indicate data where a 160 °C cut-heat was used for PH2. The open markers represent the preheat conditions chosen for equivalent dose determination i.e. where PH1 was 260 °C and PH2 was 220 °C, both held for 10 s. These data have been offset by 5 °C on the x-axis for clarity. Dashed lines represent a PH1 specific $D_e$/Mean $D_e$ ratio of 1. Y-axis tick marks are spaced at 0.1 (10%) intervals. Insufficient coarse silt-sized quartz was available to measure aliquots of 11B or 27A at a PH1 temperature of 280 °C.

## Tables

**Table S1:** AMS $^{14}C$ ages for ODP Core 658B. All ages were calibrated in Calib 7.02 using the MARINE13 radiocarbon age calibration curve (Reimer et al., 2013) with a $\Delta R$ value of 131±10 years. The upper calibrated age range for sample 29B lies beyond the calibration curve and is therefore inaccurate.

| 658B sample | Depth (m) | Lab. code | Uncalibrated age (a) | 2σ range (cal. BP) |
|---|---|---|---|---|
| 1A | 2.37 | OxA-14323 | 3165±50 | 2714-2928 |
| 3A | 2.93 | OxA-14324 | 12415±75 | 13575-13911 |
| 5B | 3.42 | OxA-14325 | 9650±120 | 10136-10678 |
| 7A | 3.90 | OxA-14326 | 11310±150 | 12334-13039 |
| 9A | 4.42 | OxA-14327 | 7990±55 | 8183-8421 |
| 11A | 4.89 | OxA-14328 | 13810±110 | 15624-16277 |
| 13B | 5.42 | OxA-14329 | 17020±110 | 19582-20166 |
| 15A | 5.92 | OxA-14330 | 20220±130 | 23357-24055 |
| 17A | 6.43 | OxA-14331 | 22930±170 | 26208-27151 |
| 19A | 6.92 | OxA-14332 | 22260±180 | 25655-26354 |
| 21A | 7.42 | OxA-14333 | 32250±450 | 35205-36016 |
| 23B | 7.93 | OxA-14334 | 37850±800 | 40235-42840 |
| 25A | 8.41 | OxA-14335 | 41300±1100 | 42578-46112 |
| 29B | 9.42 | OxA-14338 | 46300±2200 | 45196-50000 |
| 31A | 9.90 | OxA-14339 | 37000±800 | 39383-42282 |

**Table S2:** Stratigraphic markers used to construct an age model for core 658B. "AHP" is the African Humid Period and "YD" is the early AHP decrease in $CaCO_3$ content in Site 658C which deMenocal et al. (2000) equate to the Younger Dryas.

| Event | Record in which visible | Age (ka) | Reference | Depth in 659B (m) |
|---|---|---|---|---|
| AHP end | $CaCO_3$ | 5.43 | (deMenocal et al., 2000) | 2.37 |
| YD | $CaCO_3$ | 12.34 | (deMenocal et al., 2000) | 3.90 |
| AHP start | $CaCO_3$ | 14.8 | (deMenocal et al., 2000) | 4.89 |
| Maximum ice volume | $\delta^{18}O$ | 18.0 | (Lisiecki and Raymo, 2005) | 5.15 |

**Table S3:** Numbers of aliquots measured and accepted or rejected. Grain size is given in parentheses after the sample code, with "FS" indicating fine silt and "CS" indicating coarse silt. Aliquots were rejected where the recycling ratio ("Recycling") or IR depletion ratio ("IR depletion") differed from unity by more than two standard deviations, or where the sensitivity corrected luminescence intensity in response to a 0 Gy regeneration dose exceeded 5% of the sensitivity corrected natural luminescence intensity ("Recuperation").

| Sample (grain size) | Measured/Accepted | Recycling | IR depletion | Recuperation |
|---|---|---|---|---|
| 1A (FS) | 20/20 | - | - | - |
| 2A (FS) | 9/6 | 3 | - | - |
| 3A (FS) | 11/11 | - | - | - |
| 4A (FS) | 12/11 | - | - | 1 |
| 5B (FS) | 12/12 | - | - | - |
| 6A (FS) | 9/9 | - | - | - |
| 7A (CS) | 20/20 | - | - | - |
| 7A (FS) | 9/8 | 1 | - | - |
| 8A (CS) | 9/9 | - | - | - |
| 8A (FS) | 9/9 | - | - | - |
| 9A (CS) | 12/12 | - | - | - |
| 9A (FS) | 9/9 | - | - | - |
| 11A (CS) | 20/19 | 1 | - | - |
| 11A (FS) | 16/15 | 1 | - | - |
| 12A (CS) | 10/10 | - | - | - |
| 12A (FS) | 23/22 | - | 1 | - |
| 13B (CS) | 10/10 | - | - | - |
| 14A (CS) | 16/16 | - | - | - |
| 14A (FS) | 17/17 | - | - | - |
| 15A (CS) | 10/10 | - | - | - |
| 15A (FS) | 9/9 | - | - | - |
| 16A (CS) | 22/20 | 1 | 1 | - |
| 16A (FS) | 10/10 | - | - | - |
| 17A (CS) | 20/20 | - | - | - |
| 17A (FS) | 13/13 | - | - | - |
| 18A (CS) | 15/15 | - | - | - |
| 19A (CS) | 25/24 | 1 | - | - |
| 21A (CS) | 9/9 | - | - | - |
| 22A (CS) | 9/9 | - | - | - |
| 23B (CS) | 9/9 | - | - | - |
| 24A (CS) | 9/9 | - | - | - |
| 25A (CS) | 9/8 | 1 | - | - |
| 27A (CS) | 9/9 | - | - | - |
| 28A (CS) | 9/9 | - | - | - |
| 29B (CS) | 9/9 | - | - | - |
| 32A (CS) | 9/9 | - | - | - |
| 34A (CS) | 9/9 | - | - | - |
| 35A (CS) | 9/9 | - | - | - |

**Table S4:** Water and radioisotope concentrations for Core 658B samples. In addition, all samples were assumed to have $^{230}Th_{xs}$ and $^{231}Pa_{xs}$ activities of 36.6±9.3 Bq/kg and 3.38±0.87 Bq/kg at burial. These data are used to generate the dose rates presented in Tables S5-7.

| Sample | Core depth (m) | Water (%) | $^{238}U$ (ppm) | $^{232}Th$ (ppm) | K (%) |
|---|---|---|---|---|---|
| 1A | 2.37 | 57.7±5.0 | 6.33±0.39 | 5.81±0.26 | 1.10±0.08 |
| 2A | 2.65 | 57.1±5.0 | 5.88±0.36 | 4.34±0.24 | 0.72±0.05 |
| 3A | 2.93 | 56.4±5.0 | 5.14±0.29 | 3.71±0.17 | 0.57±0.04 |
| 4A | 3.15 | 55.7±5.0 | 5.71±0.34 | 3.38±0.14 | 0.46±0.03 |
| 5B | 3.42 | 54.9±5.0 | 5.69±0.33 | 4.04±0.21 | 0.42±0.03 |
| 6A | 3.65 | 54.1±5.0 | 5.74±0.31 | 3.93±0.21 | 0.40±0.02 |
| 7A | 3.90 | 53.2±5.0 | 5.60±0.29 | 4.07±0.20 | 0.68±0.05 |
| 8A | 4.15 | 52.3±5.0 | 6.82±0.40 | 4.59±0.23 | 0.52±0.03 |
| 9A | 4.42 | 51.4±5.0 | 6.07±0.35 | 3.75±0.18 | 0.45±0.04 |
| 11B | 4.89 | 49.7±5.0 | 4.38±0.24 | 3.52±0.17 | 1.00±0.06 |
| 12A | 5.15 | 48.9±5.0 | 4.15±0.21 | 4.62±0.23 | 1.10±0.06 |
| 13B | 5.42 | 48.0±5.0 | 5.13±0.30 | 4.98±0.24 | 1.11±0.06 |
| 14A | 5.65 | 47.3±5.0 | 4.78±0.30 | 4.41±0.19 | 1.09±0.06 |
| 15A | 5.92 | 46.5±5.0 | 5.20±0.28 | 5.15±0.24 | 1.18±0.07 |
| 16A | 6.15 | 45.9±5.0 | 5.09±0.29 | 4.89±0.23 | 1.19±0.08 |
| 17A | 6.43 | 45.2±5.0 | 5.08±0.30 | 5.14±0.26 | 1.25±0.07 |
| 18A | 6.65 | 44.7±5.0 | 6.12±0.32 | 6.51±0.33 | 1.19±0.07 |
| 19A | 6.92 | 44.2±5.0 | 5.89±0.35 | 5.59±0.25 | 1.28±0.08 |
| 21A | 7.42 | 43.4±5.0 | 5.28±0.30 | 4.82±0.22 | 1.10±0.06 |
| 22A | 7.65 | 43.1±5.0 | 4.27±0.20 | 5.55±0.30 | 1.16±0.07 |
| 23B | 7.93 | 42.9±5.0 | 6.03±0.35 | 4.71±0.24 | 1.11±0.07 |
| 24A | 8.15 | 42.7±5.0 | 4.76±0.25 | 4.72±0.23 | 1.14±0.06 |
| 25A | 8.41 | 42.6±5.0 | 6.47±0.36 | 5.12±0.32 | 0.83±0.05 |
| 27A | 8.93 | 42.5±5.0 | 4.86±0.27 | 5.86±0.32 | 1.14±0.07 |
| 28A | 9.15 | 42.5±5.0 | 6.02±0.32 | 4.46±0.29 | 0.80±0.05 |
| 29B | 9.42 | 42.6±5.0 | 5.27±0.28 | 4.18±0.22 | 0.75±0.05 |
| 32A | 10.19 | 43.0±5.0 | 3.72±0.23 | 5.08±0.27 | 1.03±0.07 |
| 34A | 10.65 | 43.5±5.0 | 4.76±0.27 | 5.04±0.26 | 0.92±0.06 |
| 35A | 10.92 | 43.7±5.0 | 4.92±0.16 | 5.70±0.21 | 1.02±0.06 |

**Table S5:** Equivalent dose, dose rate and age data for coarse silt samples using the Marine$_{xs}$ dose rate model. Uncertainties are based on the propagation, in quadrature, of errors associated with individual errors for all measured quantities. In addition to uncertainties calculated from counting statistics, errors due to 1) beta source calibration (3%) (Armitage and Bailey, 2005), 2) ICP-MS/Gamma spectrometer calibration (3%), 3) dose rate conversion factors (3%) and 4) attenuation factors (3%) have been included (Murray and Olley, 2002). $D_{r(supported)}$ is the dose rate due to the $^{238}U$ and $^{232}Th$ decay series in equilibrium plus the $^{40}K$ dose rate. $D_{tot(xs)}$ is the total dose due to $^{230}Th_{xs}$ and $^{231}Pa_{xs}$ since burial.

| Sample | De (Gy) | $D_{r(supported)}$ (Gy/ka) | $D_{tot(xs)}$ (Gy, total) | Age (ka) |
|---|---|---|---|---|
| 7A | 18.4±0.8 | 1.61±0.09 | 3.7±0.6 | 9.2±0.7 |
| 8A | 19.1±0.9 | 1.76±0.11 | 3.6±0.6 | 8.8±0.7 |
| 9A | 22.1±1.3 | 1.55±0.10 | 4.6±0.8 | 11.3±1.0 |
| 11B | 22.6±0.7 | 1.60±0.08 | 4.6±0.8 | 11.2±0.7 |
| 12A | 27.1±1.1 | 1.68±0.08 | 5.3±0.9 | 12.9±0.8 |
| 13B | 30.4±1.1 | 1.90±0.10 | 5.4±0.9 | 13.1±0.8 |
| 14A | 31.1±1.1 | 1.80±0.09 | 5.8±1.0 | 14.0±0.9 |
| 15A | 34.6±1.3 | 1.99±0.10 | 6.0±1.0 | 14.4±0.9 |
| 16A | 37.4±1.2 | 1.97±0.10 | 6.5±1.1 | 15.7±1.0 |
| 17A | 39.8±1.3 | 2.03±0.10 | 6.8±1.2 | 16.3±1.0 |
| 18A | 44.0±1.4 | 2.26±0.12 | 6.9±1.2 | 16.4±1.0 |
| 19A | 44.1±1.6 | 2.24±0.12 | 6.9±1.2 | 16.6±1.0 |
| 21A | 55.0±1.9 | 1.98±0.10 | 9.4±1.6 | 23.0±1.4 |
| 22A | 56.5±1.9 | 1.87±0.09 | 10.1±1.7 | 24.9±1.5 |
| 23B | 56.3±1.9 | 2.14±0.12 | 9.1±1.6 | 22.0±1.4 |
| 24A | 60.5±2.0 | 1.91±0.09 | 10.6±1.8 | 26.1±1.6 |
| 25A | 54.9±1.9 | 2.06±0.12 | 9.2±1.6 | 22.2±1.4 |
| 27A | 74.7±4.9 | 2.00±0.10 | 12.4±2.1 | 31.2±2.6 |
| 28A | 65.9±2.3 | 1.92±0.11 | 11.4±2.0 | 28.3±1.9 |
| 29B | 60.0±2.7 | 1.73±0.10 | 11.3±2.0 | 28.2±2.0 |
| 32A | 71.8±2.6 | 1.65±0.08 | 13.7±2.4 | 35.2±2.2 |
| 34A | 76.4±3.3 | 1.77±0.09 | 13.7±2.4 | 35.4±2.4 |
| 35A | 89.0±2.8 | 1.90±0.09 | 14.8±2.6 | 39.1±2.3 |

**Table S6:** Equivalent dose, dose rate and age data for coarse silt samples using the $Marine_{xs+auth}$ dose rate model. Uncertainties are based on the propagation, in quadrature, of errors associated with individual errors for all measured quantities. In addition to uncertainties calculated from counting statistics, errors due to 1) beta source calibration (3%) (Armitage and Bailey, 2005), 2) ICP-MS/Gamma spectrometer calibration (3%), 3) dose rate conversion factors (3%) and 4) attenuation factors (3%) have been included (Murray and Olley, 2002). $D_{r(sup\text{-}auth)}$ is the dose rate due to $^{238}U_{auth}$ in equilibrium to $^{234}U$ and the $^{238}U_{detrital}$ and $^{232}Th$ decay series in equilibrium plus the $^{40}K$ dose rate. $D_{tot(xs)}$ is the total dose due to $^{230}Th_{xs}$ and $^{231}Pa_{xs}$ since burial.

| Sample | De (Gy) | $D_{r(sup\text{-}auth)}$ (Gy/ka) | $D_{tot(xs)}$ (Gy, total) | Age (ka) |
|---|---|---|---|---|
| 7A | 18.4±0.8 | 0.98±0.10 | 5.3±0.9 | 13.4±1.3 |
| 8A | 19.1±0.9 | 0.98±0.12 | 5.5±0.9 | 13.8±1.5 |
| 9A | 22.1±1.3 | 0.84±0.11 | 7.0±1.2 | 17.9±2.1 |
| 11B | 22.6±0.7 | 1.11±0.08 | 6.0±1.0 | 14.9±1.2 |
| 12A | 27.1±1.1 | 1.26±0.08 | 6.6±1.1 | 16.3±1.2 |
| 13B | 30.4±1.1 | 1.35±0.10 | 7.0±1.2 | 17.3±1.3 |
| 14A | 31.1±1.1 | 1.28±0.09 | 7.5±1.3 | 18.4±1.4 |
| 15A | 34.6±1.3 | 1.43±0.10 | 7.7±1.3 | 18.9±1.4 |
| 16A | 37.4±1.2 | 1.41±0.10 | 8.4±1.4 | 20.6±1.6 |
| 17A | 39.8±1.3 | 1.48±0.10 | 8.6±1.5 | 21.1±1.5 |
| 18A | 44.0±1.4 | 1.61±0.12 | 8.9±1.5 | 21.8±1.6 |
| 19A | 44.1±1.6 | 1.59±0.12 | 9.0±1.6 | 22.1±1.7 |
| 21A | 55.0±1.9 | 1.38±0.10 | 12.2±2.1 | 30.9±2.4 |
| 22A | 56.5±1.9 | 1.44±0.09 | 12.1±2.1 | 30.7±2.1 |
| 23B | 56.3±1.9 | 1.42±0.12 | 12.2±2.1 | 30.9±2.6 |
| 24A | 60.5±2.0 | 1.38±0.10 | 13.3±2.3 | 34.1±2.5 |
| 25A | 54.9±1.9 | 1.30±0.12 | 12.8±2.2 | 32.5±2.9 |
| 27A | 74.7±4.9 | 1.50±0.10 | 15.2±2.6 | 39.8±3.6 |
| 28A | 65.9±2.3 | 1.20±0.12 | 15.8±2.7 | 41.9±3.8 |
| 29B | 60.0±2.7 | 1.10±0.10 | 15.4±2.7 | 40.5±3.8 |
| 32A | 71.8±2.6 | 1.29±0.08 | 16.1±2.8 | 43.0±3.1 |
| 34A | 76.4±3.3 | 1.26±0.09 | 17.2±3.0 | 47.0±3.8 |
| 35A | 89.0±2.8 | 1.39±0.09 | 18.3±3.2 | 51.0±3.6 |

**Table S7:** Equivalent dose, dose rate and age data for fine silt samples using the $Marine_{xs+auth}$ dose rate model. Uncertainties are based on the propagation, in quadrature, of errors associated with individual errors for all measured quantities. In addition to uncertainties calculated from counting statistics, errors due to 1) beta source calibration (3%) (Armitage and Bailey, 2005), 2) ICP-MS/Gamma spectrometer calibration (3%), 3) dose rate conversion factors (3%) and 4) attenuation factors (3%) have been included (Murray and Olley, 2002). $D_{r(sup\text{-}auth)}$ is the dose rate due to $^{238}U_{auth}$ in equilibrium to $^{234}U$ and the $^{238}U_{detrital}$ and $^{232}Th$ decay series in equilibrium plus the $^{40}K$ dose rate. $D_{tot(xs)}$ is the total dose due to $^{230}Th_{xs}$ and $^{231}Pa_{xs}$ since burial.

| Sample | De (Gy) | $D_{r(sup\text{-}auth)}$ (Gy/ka) | $D_{tot(xs)}$ (Gy, total) | Age (ka) |
|---|---|---|---|---|
| 1A | 8.65±0.29 | 1.48±0.14 | 2.1±0.4 | 4.4±0.4 |
| 2A | 14.90±0.92 | 1.10±0.13 | 4.5±0.9 | 9.5±1.1 |
| 3A | 18.51±1.26 | 0.92±0.11 | 6.2±1.2 | 13.3±1.6 |
| 4A | 22.56±0.72 | 0.86±0.12 | 7.8±1.5 | 17.1±2.0 |
| 5B | 22.32±1.10 | 0.90±0.12 | 7.6±1.5 | 16.4±2.0 |
| 6A | 28.99±1.07 | 0.88±0.12 | 9.8±1.9 | 21.7±2.5 |
| 7A | 29.08±1.07 | 1.07±0.12 | 8.8±1.7 | 18.9±2.0 |
| 8A | 25.68±0.99 | 1.09±0.15 | 7.8±1.5 | 16.5±1.9 |
| 9A | 38.81±1.47 | 0.94±0.13 | 12.6±2.5 | 28.0±3.4 |
| 11B | 48.56±1.83 | 1.29±0.15 | 12.6±2.5 | 27.8±2.9 |
| 12A | 62.53±2.58 | 1.19±0.10 | 16.7±3.3 | 38.5±3.5 |
| 13B | 62.91±2.53 | 1.35±0.10 | 15.6±3.0 | 35.1±2.9 |
| 14A | 66.57±2.23 | 1.37±0.12 | 16.3±3.2 | 36.6±3.2 |
| 15A | 65.89±2.39 | 1.54±0.12 | 15.1±2.9 | 33.1±2.8 |
| 16A | 52.49±2.01 | 1.52±0.13 | 12.5±2.4 | 26.4±2.3 |
| 17A | 58.51±2.00 | 1.59±0.13 | 13.4±2.6 | 28.5±2.4 |

**References**

Armitage, S.J., Bailey, R.M., 2005. The measured dependence of laboratory beta dose rates on sample grain size. Radiat Meas 39, 123-127.

deMenocal, P., Ortiz, J., Guilderson, T., Adkins, J., Sarnthein, M., Baker, L., Yarusinsky, M., 2000. Abrupt onset and termination of the African Humid Period: Rapid climate responses to gradual insolation forcing. Quaternary Science Reviews 19, 347-361.

Lisiecki, L.E., Raymo, M.E., 2005. A Pliocene-Pleistocene stack of 57 globally distributed benthic δ 18O records. Paleoceanography 20, 1-17.

Murray, A.S., Olley, J.M., 2002. Precision and accuracy in the optically stimulated luminescence dating of sedimentary quartz: a status review. Geochronometria 21, 1-16.

Reimer, P.J., Bard, E., Bayliss, A., Beck, J.W., Blackwell, P.G., Bronk Ramsey, C., Buck, C.E., Cheng, H., Edwards, R.L., Friedrich, M., Grootes, P.M., Guilderson, T.P., Haflidason, H., Hajdas, I., Hatté, C., Heaton, T.J., Hoffmann, D.L., Hogg, A.G., Hughen, K.A., Kaiser, K.F., Kromer, B., Manning, S.W., Niu, M., Reimer, R.W., Richards, D.A., Scott, E.M., Southon, J.R., Staff, R.A., Turney, C.S.M., van der Plicht, J., 2013. IntCal13 and Marine13 radiocarbon age calibration curves 0-50,000 years cal BP. Radiocarbon 55, 1869-1887.